

Biogeochemical cycles Mediterranean Sea climatologies and budget

Table des matières

1. Introduction.....	57
2. Methodology.....	59
2.1. The physical model.....	59
2.2. The biogeochemical model.....	60
2.3. Implementation on the Mediterranean basin.....	61
2.3.1. Biological boundary conditions.....	61
2.3.2. Initialization and spin up.....	62
3. Results and discussion.....	62
3.1. Evaluation of the model.....	63
3.1.1. Surface chlorophyll.....	64
3.1.2. Biogeochemical characteristics of water masses.....	67
3.2. Climatology.....	69
3.2.1. Mixed layer depth.....	69
3.2.2. Depth and magnitude of the Deep Chlorophyll Maximum (DCM).....	71
3.2.3. Nutriclines.....	74
3.2.4. Net primary production (NPP).....	76
3.2.5. Organic carbon export.....	78
3.3. Main pelagic ecological regimes of the Mediterranean Sea.....	80
3.3.1. Bloom like regime (group 1).....	82
3.3.2. No-bloom regime of the western basin (group 3).....	83
3.3.3. No-bloom regimes of the eastern basin (groups 4, 5, 6).....	85
3.3.4. The Intermittent/Intermediate regime (group 2).....	85
3.4. Nitrogen and phosphorus dynamics in the Mediterranean Sea.....	87
3.4.1. Biogeochemical processes.....	87
3.4.2. Fluxes at the straits.....	88

3.4.3. The global budget.....	89
4. Conclusion and perspectives.....	92

Authors

F. Kessouri¹, C. Ulses¹, P. Marsaleix¹, J. Beuvier^{2,3}, S. Somot³, F. D’Ortenzio^{4, 5}, M. Pujo-Pay^{6, 7}, L. Prieur⁵, C. Estournel¹

¹ Laboratoire d’Aérodologie, UMR 5560 CNRS, Université de Toulouse 3, 14 avenue Edouard Belin, 31400 Toulouse, France

² Mercator Océan, 10 rue Hermès, 31520 Ramonville-Saint-Agne, France

³ Météo France, 42 av. Gaspard Coriolis, 31057 Toulouse CEDEX, France

⁴ Sorbonne Universités, UPMC Univ Paris 06, UMR 7093, Laboratoire d’Océanographie de Villefranche, 06230 Villefranche-sur-Mer, France

⁵ CNRS, UMR 7093, LOV, 06230 Villefranche-sur-Mer, France

⁶ Sorbonne Universités, UPMC Univ Paris 06, UMR 7621, Laboratoire d’Océanographie Microbienne, Observatoire Océanologique, Avenue du Fontaulé, 66650 Banyuls/mer, France

⁷ CNRS, UMR 7621, Laboratoire d’Océanographie Microbienne, Observatoire Océanologique, 66650 Banyuls/mer, France

Key points up to three (<100 characters)

- Decadal study using high resolution physical-biogeochemical model
- Biogeochemical climatologies based on modeling
- Ecological regionalization
- Mediterranean budgets of nitrogen and phosphorus

Abstract

The Mediterranean Sea is characterized by complex climatic characteristics, a well-developed thermohaline circulation at the scale of the western and eastern basins and energetic gyre and jet systems at sub-basin scale. These characteristics impact on the hydrological, biogeochemical and biological water mass properties. A ten years 1/12° offline simulation of the biogeochemical cycles of the Mediterranean Sea was performed using the ECO3M-S biogeochemical model and the daily averaged physical fields computed by the NEMO OGCM. The simulation is analyzed according to three thematic axes.

The first axis is a monthly climatology of mixed-layer depth and biogeochemical characteristics describing

the seasonal cycles at sub-basins scale and the impact of key processes (such as deep-convection or seasonal stratification) on the nutriclines and DCM depth or biogenic inputs in the surface layer. The second axis is a regionalization based on physical and biogeochemical parameters leading to the identification of seven bioregions and four main trophic regimes, namely, the deep-convection regime (and ensuing phytoplankton blooms), the intermediate mixing regime, and the stratified regimes in the western and eastern basins. The third axis proposes a biogeochemical budget based on nitrogen and phosphorus fluxes through the straits and on transfers between organic and inorganic forms. At the Gibraltar strait, the inorganic nitrogen outflow is about $140 \cdot 10^9$ moles per year while the organic inflow is about $80 \cdot 10^9$ moles per year. The western basin is globally a source of organic matter, a substantial part of which is exported to the eastern basin. The eastern basin is a source of inorganic matter, a part of which is exported to the western basin by the circulation of the Levantine Intermediate Water.

1. Introduction **Biogeochemical cycles of the Mediterranean Sea:** **climatologies and budget**

The semi-enclosed Mediterranean Sea is driven by global dynamics forced by climate and thermohaline cyclonic circulation. Local regional dynamics impact on water masses properties and biological activity, as well as the amount of chemicals. An accurate budget of the Mediterranean needs accurate components of the water budget (inflows and outflows at the straits, runoff and precipitation) and an accurate determination of concentrations in these external inputs and in the different water masses. Budget of nutrients and processes analysis are the keys to understand biological ecosystem behavior. Front lines which meet these problematics were the work exposed in (Bethoux et al., 1988, Bethoux et al. 1990; Bethoux and Gentili, 1996; Bethoux, 1998).

Main biological processes were already well described in previous models. Lazzari et al., (2012), based on the “Longhurst biological classification” (Longhurst, 1995), qualified Mediterranean Sea as a “subtropical nutrient-limited winter spring production period bioregion” in adequacy with chlorophyll profiles exposed by (Lavigne et al., 2015; Mignot et al., 2014), where subsurface chlorophyll distribution in the Mediterranean Sea corresponds to some other subtropical regions. (Lazzari et al., 2012) have summarized the spatial gradient of net primary production (NPP) and its strong seasonal cycle over the basin. They demonstrated that this production depends on surface and integrated water properties. Crise et al., (1998) have mentioned west to east deepening of the nitracline, going from 50 m in Alboran Sea until 110m in Levantine Sea. Deep

chlorophyll maximum (DCM) is globally superimposed on the nutriclines as studied by Macías et al., (2014). These authors have exposed that the DCM accounts for an important part of NPP and covers about 95% of the basin during the long oligotrophic period. Lavigne et al., (2015) thanks to a calibration of fluorescence derived chlorophyll of large historical datasets demonstrated that DCM should be estimated deeper than mentioned by Macías et al., (2014) and gave an estimation of a gradual deepening of DCM of 1.6m per longitudinal degree during stratified conditions.

Coupled physical/biogeochemical models meet limits because. Some limits are related to their physical component and associated atmospheric forcing. For example, a deeper MLD may cause an increased enrichment of surface waters. In contrary, weaker MLD than expected may cause a higher surface oligotrophy. Other problems may be linked to the calibration of biogeochemical model parameters which is difficult to obtain all over an area composed of regions with different biogeochemical functioning. The Mediterranean Sea is very heterogeneous and contains a large number of bioregions each one with its own biological functioning. Based on phytoplankton annual cycle, D'Ortenzio et al., (2009) classified the Mediterranean Sea into three groups: first, "Bloom-Like regime" characterized by quick and intense spring bloom. Then, "intermittent regime" characterized by long phytoplankton winter efflorescence and "NO-Bloom regime" present low chlorophyll concentration and their cycle seems like doming. To our knowledge, there are no coupled models able to represent these different trophic regimes.

Another important problem of modelling is related to the initialization and boundary forcing. Indeed, time of simulation is of the order of the decade which is much lower than the residence time of water masses (Millot, 2005). Therefore specific initialization is required to attempt in short time the physical and the biogeochemical equilibrium states.

As mentioned by Macías et al., (2014), biological inputs from rivers, Atlantic and Black seas, and atmosphere suffer from large uncertainties. Important failures could be seen in shallow waters of western part of Alboran Sea, the Adriatic Sea and in the Gulf of Gabès.

Using modeling, this paper aims to describe the most important biogeochemical properties of the whole Mediterranean Sea, by identifying geographical distribution of each of them. An annual budget of biogenic matter circulating in the basin over the straits of Gibraltar and Sicily is also presented.

The paper is organized as follows: First the second section presents the modelling based methodology used

in this study. Then results are presented in the third section, such as climatologies of the physical properties, together with climatologies of biogeochemical surface and water body properties, on the whole Mediterranean on a monthly climatological basis. Biogeochemical processes in four main regimes are quantified derived from a statistical clustering method, then discussed. A global nitrogen budget and nutrient fluxes at the Mediterranean straits are then presented to conclude the discussion. Conclusions and perspectives are given in the fourth section.

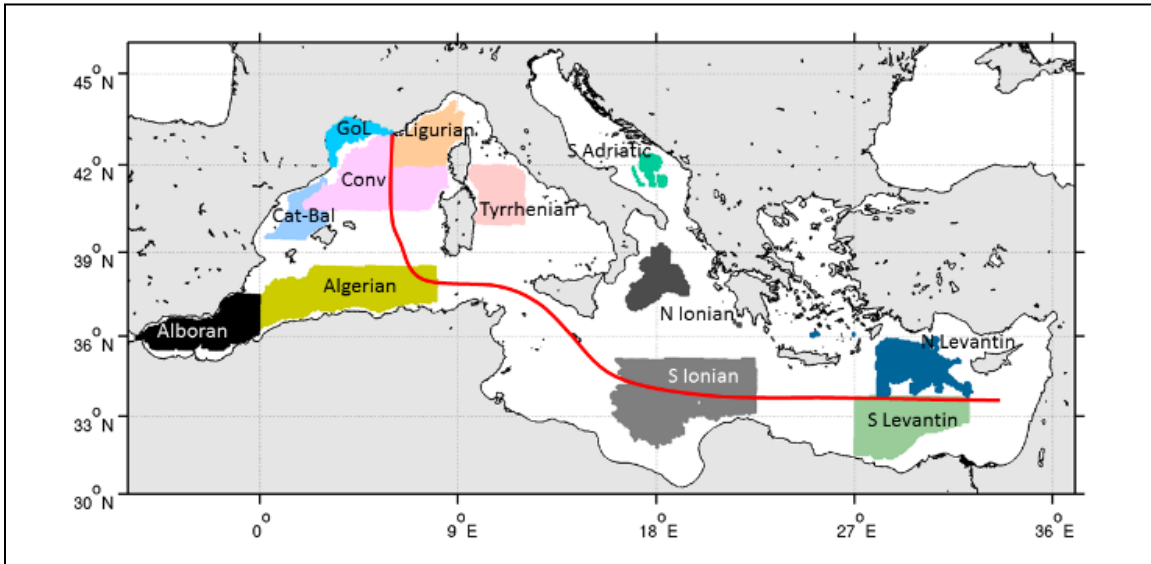


Figure 1: Position of the averaged regions in the chlorophyll validation section. Red line represents the transect performed by the oceanographic cruise BOUM in June and July 2008.

2. Methodology

In this study we have used a 3D coupled physical biogeochemical modeling. The biogeochemical multi-elements Eco3M-S model (Auger et al., 2011, 2014), has been forced offline by the outputs of the hydrodynamic NEMO-MED12 model (Hamon et al., in revision) resolving mesoscale processes, via the BLOOM platform (pers. comm. P. Marsaleix).

2.1. The physical model

The configuration of the ocean general circulation NEMO model used was the regional configuration of the Mediterranean Sea, NEMO-MED12 (Hamon et al., in press), with a $1/12^\circ$ (~ 7 km) horizontal resolution and

75 vertical z-levels with partial steps. The domain of modeling is indicated in Figure 1. It covers the whole Mediterranean Sea and a buffer zone west of the Strait of Gibraltar. The simulation, called NM12-FREE, described in (Hamon et al., in press) is a free run (i.e. without data assimilation) that starts in October 1979 and ends in June 2013. Initial conditions were provided by the monthly mean potential temperature and salinity 3-D fields from the state of the MEDATLAS-1979 climatology (Rixen et al., 2005) in the Mediterranean side and, in the Atlantic side, from the global ocean reanalysis ORAS4 (Balmaseda et al., 2013) at the same date. The exchanges with the Atlantic basin were performed through the buffer zone where 3-D temperature, salinity and sea level were relaxed toward ORAS4 monthly fields. River inputs were taken into account based on the climatological average of the dataset of Ludwig et al. (2009). For the 33 main rivers, the runoff values of the dataset were prescribed while for the other rivers, the value of runoff corresponded to an average in each subbasin. The Black Sea was not included in the model domain but represented a major source of freshwater. It was considered as a river for the Aegean Sea at the Dardanelles Strait. The model is forced by the 3-hourly atmospheric fluxes from an ALADIN-Climate simulation at 12 km of resolution (Herrmann et al., 2010), driven by the ERA-Interim atmospheric reanalysis, and called ALDERA (Hamon et al., in revision).

2.2. The biogeochemical model

The biogeochemical Eco3M-S model is a multi-nutrient and multi-plankton functional type model (Auger et al., 2011). It describes the cycles of C, N, P and Si. This model was previously used to study the multi-annual ecosystem variability in the NW Med (Auger et al. 2014; Herrmann et al. 2013) and the ecosystem functioning in the Gulf of Lions shelf influenced by the Rhone river inputs. We have re-calibrated the previous version described in Auger et al. (2014) in order to implement the model on the whole Mediterranean Sea. The different recalibrated parameters are described in (Kessouri et al., in prep-b). Eco3M-S consists of seven interconnected compartments (Fig. 2): (1) The inorganic compartment representing nitrate, ammonium, phosphate and silicate, (2) the dissolved organic matter compartment considered under the forms of carbon, nitrogen and phosphorus (3) particulate organic matter compartment (under the forms of C, N, P, Si and chlorophyll), divided in two weight classes, light and heavy, (4) the autotrophic compartment composed of three classes of phytoplankton classified by size: pico-phytoplankton (smaller than 2 microns, nano-phytoplankton (between 2 and 20 microns), and micro-phytoplankton (between 20 and 200 microns) that corresponds in the model to diatoms, (5) the zooplankton compartment composed of three size classes of zooplankton: nano-zooplankton [diameter < 20 μ m], micro-zooplankton [20 μ m > diameter > 200 μ m] and meso-zooplankton [diameter > 200 μ m] and (6) the bacteria compartment. The relative internal composition,

i.e. the stoichiometry, of each functional type is considered as variable for autotrophic organisms and constant for heterotrophic organisms. (7) Oxygen: Oxygen is consumed by plankton and bacteria; it is also produced inside the water mass through phytoplankton photosynthesis. Air-sea exchanges are performed throughout Wanninkhof and McGillis (1999) laws.

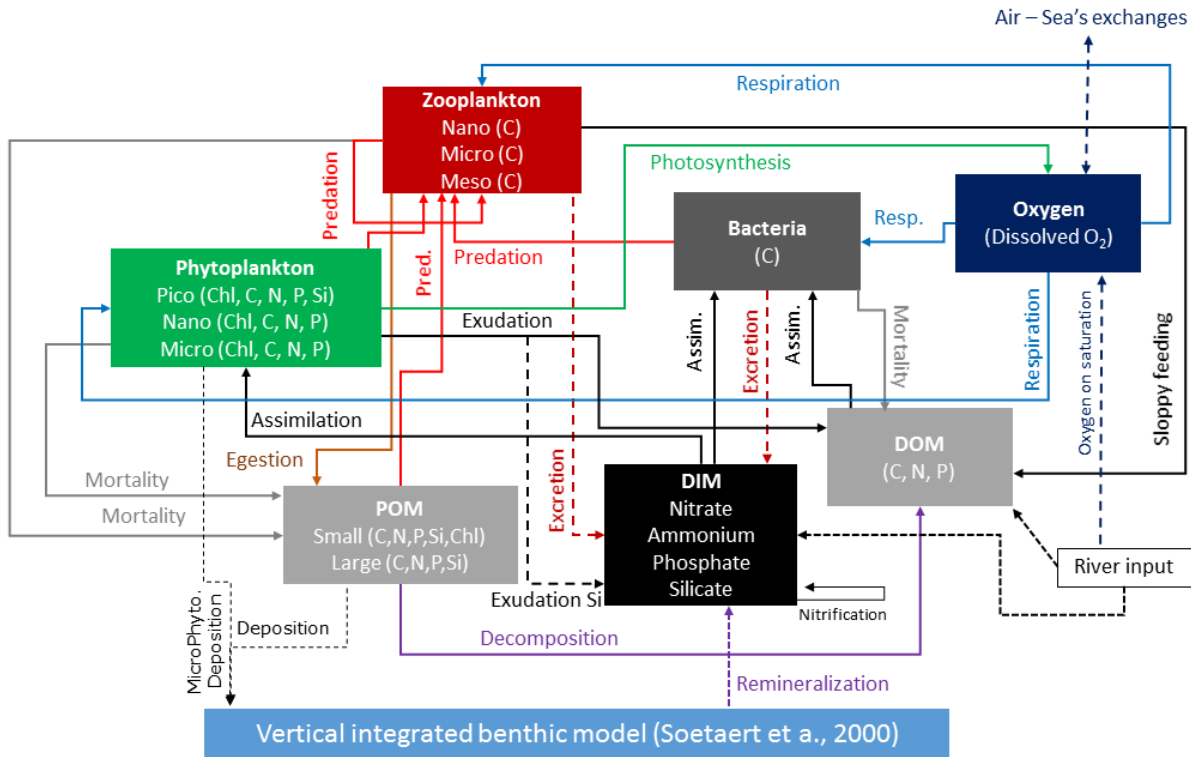


Figure 2: Scheme of the biogeochemical model Eco3m-S

2.3. Implementation on the Mediterranean basin

2.3.1. Biological boundary conditions

In the Atlantic Ocean, nutrients and oxygen have been prescribed using monthly profiles from “World Ocean Atlas 2009” climatology at 7.5° W. This boundary condition’s limit has been chosen close to the Strait of Gibraltar to avoid spurious effects caused by relaxation on physical parameters in the buffer zone.

The Black Sea was not included in the model domain but it represents a major source of freshwater. It was considered in the NEMO-MED12 configuration as a river for the Aegean Sea at the Dardanelles Strait. At this strait, constant values for organic matter have been applied according to Copin Montegut (1993). Nutrient

inputs have not been introduced at the Dardanelles Strait because of the null net flow (Tugrul et al., 2002).

At the runoff points, concentrations of nutrients have been imposed by region using dataset of Ludwig et al. (2010). As organic matter concentrations in the continental waters are most often unknown, constant values derived from the historical dataset of the Rhône River at Arles station (MOOSE program, pers. comm. Raimbault) have been imposed for these inputs.

At the sea surface, atmospheric deposition of inorganic matter has been prescribed as constant values for western (west to Sicily Strait) and eastern sub-basins based on “low” estimations reported by Ribera d’Alcalà et al. (2003). Deposition of organic matter has been deduced from relationships between inorganic and organic matter deduced from MOOSE network data collected south of France (pers. comm. Raimbault).

Nutrient fluxes at the water column/sediment interface have been obtained through a coupling of the biogeochemical model with a simplified version of the vertically-integrated benthic model described by Soetaert et al. (2000).

2.3.2. Initialization and spin up

In previous Mediterranean Sea modelling studies, initialization states were based either on climatology (Crise et al., 1998; Crispi et al., 2002) or, at sub-basin scale, on relationships between nutrients and physical properties of water masses (Priour and Legendre, 1988; Auger et al., 2014). In this study, inorganic variables have been initialized using the historical database defined in 13 regions by Lavezza et al. (2011). Depending on the amount and spatial distribution of nutrients and hydrological salinity profiles in each bio-region, we have chosen one type of initialization mentioned above: we have used relations linking nutrients to salinity in the upper layer and intermediate waters, then a constant value in the deeper layer in the western basin where profiles are numerous and allow a seasonal description. In the eastern basin, because of the lack of the combined biological and physical datasets near coastal zones we have deduced nutrients’ median profiles in each region defined by Lavezza et al. (2011).

The spin-up of a model is an important issue as its stability is required to calculate reliable budgets. Stable nutrient and organic matter stocks on the whole the basin have been obtained after four years of simulation (for instance, the total nitrate stock presents an annual variability around 0.05 %). Thus, the simulation has been started in 2000 using the final state of a first 2000-2004 simulation. It ends in 2013. In this paper we focus on the period 2003 – 2013.

3. Results and discussion

This section is divided in four parts:

First, we present an evaluation (1) of simulated surface chlorophyll patterns using daily 4km resolution outputs of MODIS Aqua satellite products and (2) of water mass properties, focusing on nutrient chlorophyll and DOC concentrations over the basin, based on the trans Mediterranean BOUM cruise dataset (Pujo-Pay et al., 2011; Moutin and Prieur, 2012) occurring in summer 2008. To address the lack of temporal comparison, especially in winter, values were reported and compared to experiences mentioned in literature in the Gulf of Lions, in the Adriatic Sea and in the Rhodes Gyre.

In the second part, the monthly climatologies of hydrological and biogeochemical parameters calculated over the [2003 – 2013] decade from model outputs are presented and discussed.

In the third part, the functioning of four kinds of regimes is described throughout clustering analysis using models output using selected parameters. Finally, matter exchanges and flux at the straits of the Mediterranean Sea and biological fluxes in the eastern and the western basins are highlighted.

3.1. Evaluation of the model

3.1.1. Surface chlorophyll

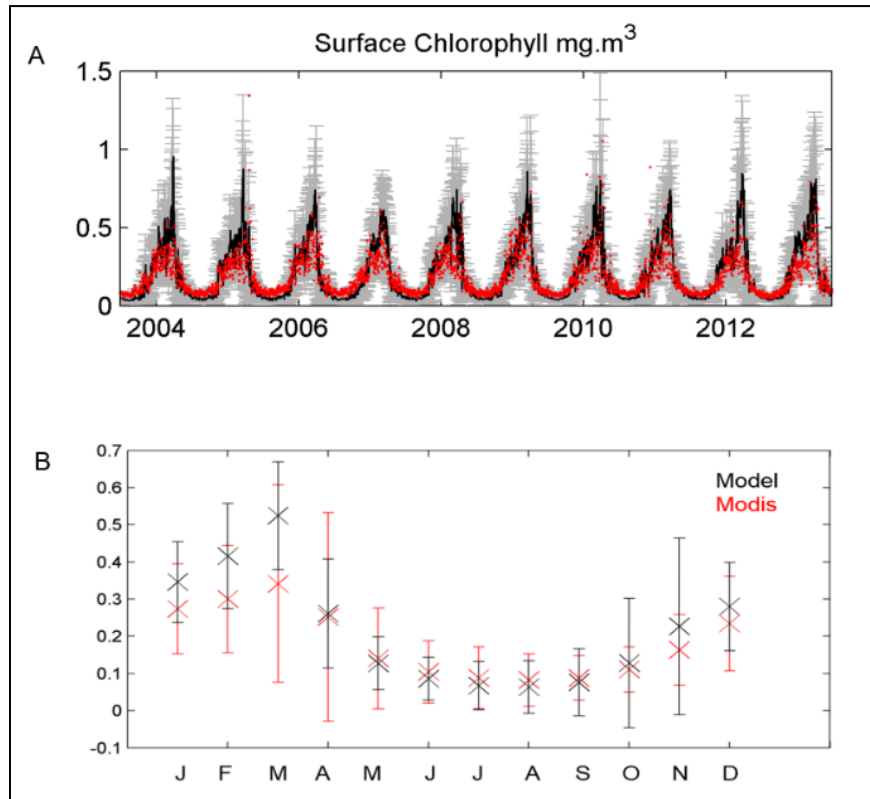


Figure 3: A. Observed (MODIS at 4 km resolution, in black) and modeled (red) surface chlorophyll concentration (mg m^{-3}) averaged over the whole Mediterranean basin Grey points represent standard deviation in model outputs. B. Modeled (black) and observed (red) monthly average and standard deviation of surface chlorophyll concentration.

Figure 3-A presents a comparison between simulated (without considering penetration depth) and observed surface chlorophyll concentrations averaged over pelagic areas (bathymetry > 500m) of the whole basin from summer 2003 to summer 2013. Model results show a good agreement in the temporal evolution with the observations. The Spearman correlation coefficient between data and model outputs is equal to 0.93 ($p < 0.01$). The difference between model outputs and observations is maximum in winter (January, February and March) when the mean concentration is strong (Fig. 3-B). Its annual mean value is equal to 0.02 mg.m^{-3} . The timing of the maximum is also generally well represented except in some cases where it is anticipated by about 5 to 7 days as in 2005. Statistics (mean, RMSD, standard deviation) concerning each subbasin (Fig. 1) are presented in Tab. 1. The mean concentration for each subbasin is very close between observations and model outputs. However, the standard deviation in model outputs are higher than in observations and

RMSD (Friedrichs et al., 2009) higher than the mean values in eastern regions.

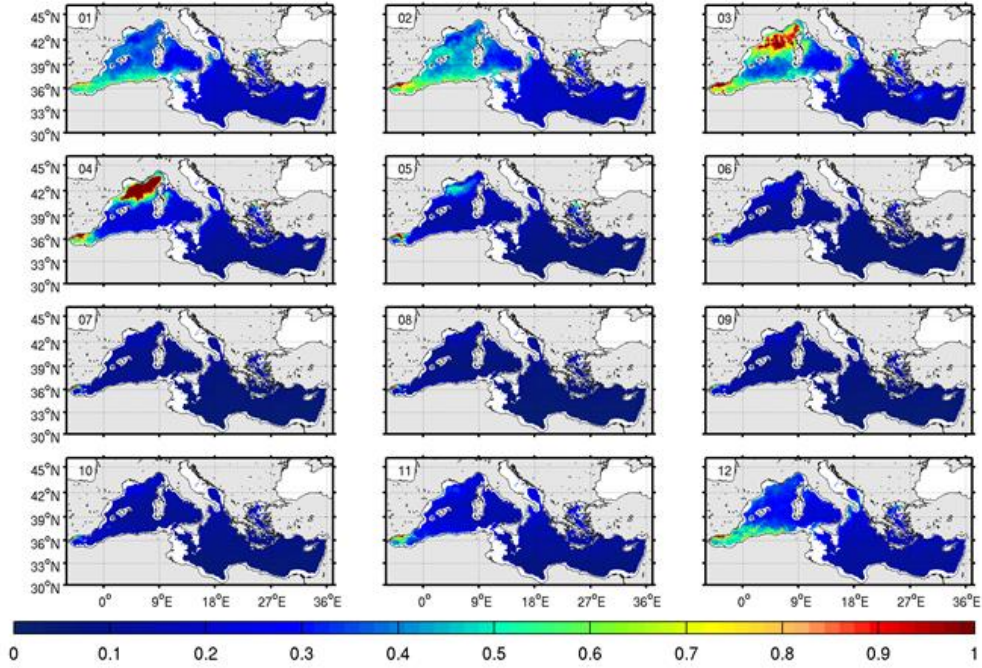
Regions	Alboran	Algerian	Conv.	Ligurian	Cat-Bal	Adriatic	N Ionian	S Ionian	N Levantin	S Levantin
STD obs	0.35	0.18	0.36	0.34	0.19	0.10	0.07	0.05	0.06	0.04
STD mod	0.31	0.23	0.37	0.36	0.32	0.23	0.19	0.12	0.18	0.12
MEAN obs	0.43	0.24	0.33	0.32	0.26	0.18	0.13	0.09	0.10	0.07
MEAN mod	0.38	0.26	0.33	0.32	0.30	0.14	0.13	0.10	0.13	0.08
RMSD obs vs mod	0.34	0.13	0.31	0.31	0.23	0.20	0.15	0.08	0.14	0.09

Table 1: Statistics of surface chlorophyll from the model and from Modis by region showed in Fig. 1.

Figure 4 displays a comparison between observed and simulated monthly surface chlorophyll concentration 2D fields. The model reproduces correctly the East-West and South-North concentration gradients. Seasonal variability in each region is well reproduced. Chlorophyll concentration is generally maximal during winter (in the whole basin except in the north-western subbasin) or spring (in the north-western subbasin), and low during the long oligotrophic period, from May until October. The model reproduces correctly the autumn (November – December) efflorescence observed by satellite particularly in the western basin. Nevertheless, an overestimation of $0.4 \text{ mg}\cdot\text{m}^{-3}$ is noteworthy in the south Adriatic, northern Ionian and northern Levantine subbasins in February and March. This difference could be caused by an overestimation of the deepening of the mixed layer as it will be seen in section 3.2.1. In contrary, the Alboran Sea is less productive in the model than in the observations. This default could be due to the fact that we didn't take into account tides that could favor nutrients upwelling through increased vertical diffusivities (Sanchez-Vidal et al., 2008; Renault et al., 2012). An underestimation of chlorophyll in the model is also visible along the African coast in the thin Algerian current, which is weaker in the model than in the estimations performed by Millot (1999) based on

MEDIPROC data set.

MODIS 4Km Surface Chla [2003-2013] (mg/m3)



Surface Chla [2003-2013] (mg/m3)

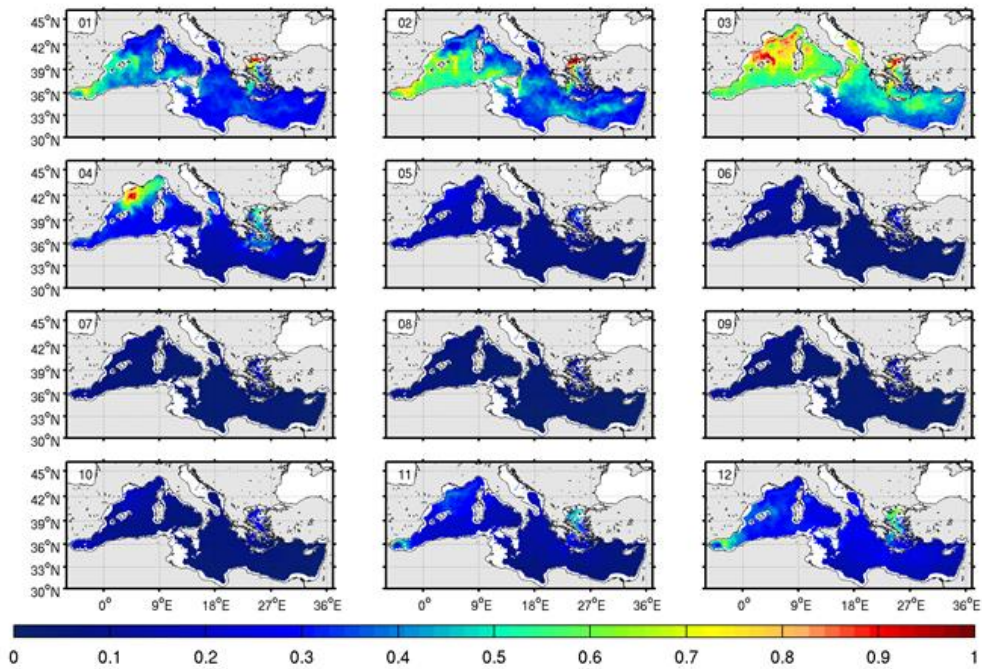
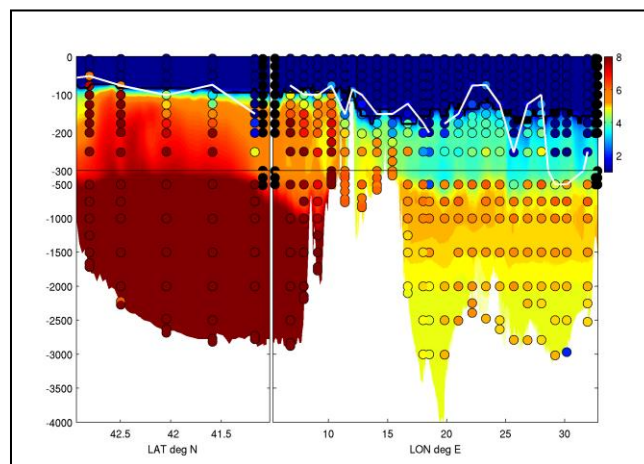


Figure 4: 10-year (2003-2013) average of observed (top) and modeled (down) monthly surface chlorophyll concentrations

3.1.2. Biogeochemical characteristics of water masses

The ability of the model to represent the biogeochemical characteristics of the different water masses has been evaluated through a confrontation of model results against the observations of the BOUM cruise (Moutin & Prieur, 2012) along transects from North to South in the western basin and from West to East in the eastern basin (indicated on Figure 1). The cruise lasted for one month and a half between June and July 2008. We have averaged the model outputs during the period of the cruise (July to August 2008).

Over the entire transect, observed and simulated nutrients (nitrate and phosphate) show extremely low concentrations in the surface layer (Fig. 5). Nitracline has been defined here as the depth where nitrate is equal to 1 mmol.m^{-3} , and for the phosphocline the threshold concentration has been chosen equal to 0.05 mmol.m^{-3} (Lazzari et al., 2012). As in the observations, nitracline is localized at 60 m depth in the western basin and gradually deepens to attain 120 m in the eastern Levantine basin. Phosphocline is close to the nitracline in the western basin but a gradual decoupling between both nutriclines is then observed to the east. The difference between both depths could reach 40 m in some locations in the eastern part of the Levantine Sea.



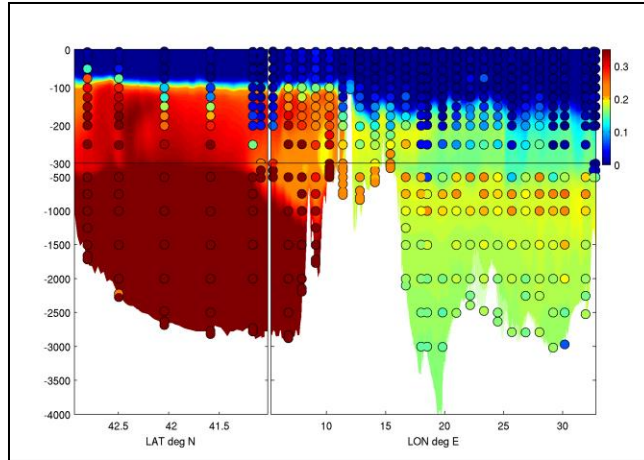


Figure 5: Left panel Nitrate concentration [mmol.m^{-3}] comparison, between model's outputs (background) and BOUM transect observations (dots). Same for phosphate in the right panel. Black dots are missed data in the left panel.

In the eastern sub-basin, local deepening of the nutriclines are observed at some stations, due to the presence of anticyclonic eddies (Moutin and Prieur, 2012). This pattern is represented in model outputs but it is not clearly visible in the modeled averaged outputs presented in Figure 5. The model reproduces maximum concentrations of nitrate ($\sim 5.5 \text{ mmol.m}^{-3}$) and phosphate ($\sim 0.25 \text{ mmol.m}^{-3}$) observed in the intermediate waters (250 - 500m) in the eastern basin. Nevertheless, these maxima are slightly underestimated (by 0.5 mmol.m^{-3} for nitrate, and 0.05 mmol.m^{-3} for phosphate). In the western basin below the nutriclines, concentrations increase from 1 to 7 mmol.m^{-3} for nitrate, and from 0.05 to 0.3 mmol.m^{-3} for phosphate in less than 100 m. However, intermediate waters seem to be less concentrated in the model by a gap of about $\sim 0.5 \text{ mmol.m}^{-3}$ for nitrate and $\sim 0.025 \text{ mmol.m}^{-3}$ for phosphate in some western zones. For instance, the deepening of the nitracline is more important at the latitude 41 which is not represented in the model. Like observations, modeled deep water masses are characterized by values higher than 8 mmol.m^{-3} for nitrate, and higher than 0.4 mmol.m^{-3} for phosphate as also observed by (Béthoux et al., 1998; Pujó-Pay et al., 2011; Severin et al., 2014).

Simulated deep chlorophyll maximum (DCM, showed in figure 6) deepens from West to East as the nutriclines. The depth of the DCM is around 55 m in the north-west region and gradually attains 110 m near the eastern boundary of the transect in the central Levantine sub-basin. Observation and modeled data have the same patterns.

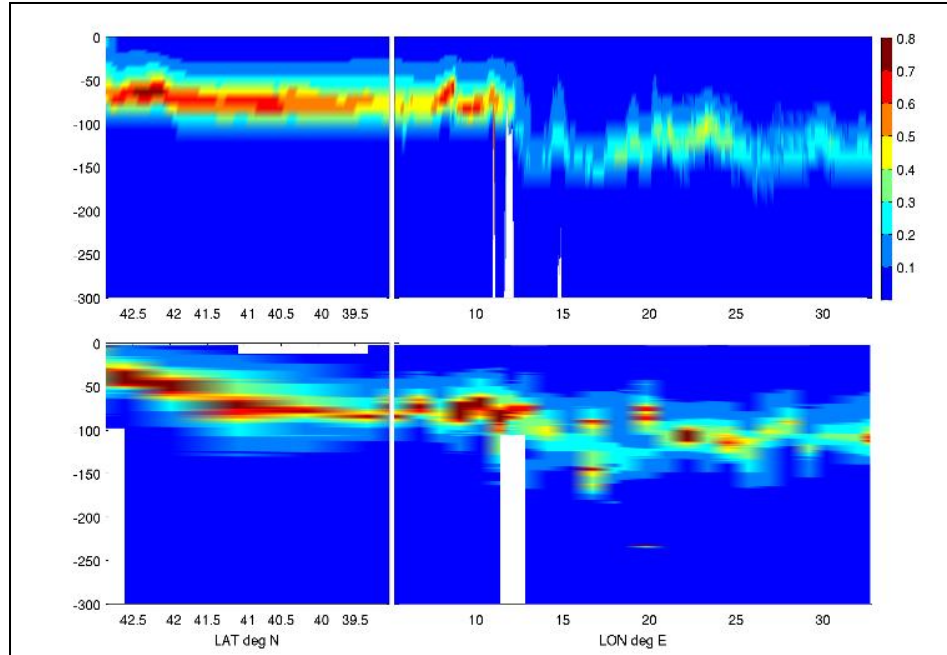


Figure 6: Chlorophyll [mgChl/m^3] (zoom 0-300m depth) comparison between model (upper) and BOUM in situ data (lower).

3.2. Climatology

First, climatologies of the mixed layer depth (MLD) are presented. Then we present a climatology for biogeochemical properties (DCM, nutriclines, amount of nitrate in the top 150m layer and surface oxygen concentration) and biological fluxes (net primary production or organic carbon export).

3.2.1 Mixed layer depth

The MLD has been defined here as the depth where the potential density increases by $0.01 \text{ kg}\cdot\text{m}^{-3}$ relatively to the 10 m depth. The climatology of the MLD (Fig. 7) shows two key periods. The first period is a vertical mixing season between October and April and the second one is a stratified period between May and September. During winter, only coastal regions (not shown) under the influence of freshwater discharges as well as the North Aegean influenced by the inflow of the Black Sea present a thin MLD.

The thickest MLD are found in February. The patterns of thick MLD ($> 100 \text{ m}$) are generally close to those presented by Houpert et al. (2015) in its climatology based on *in situ* observations. They are located in the Gulf of Lions and the Tyrrhenian Sea for the western basin, the south Adriatic and North Ionian Sea for the

central basin and the Levantine Sea for the Eastern basin. Among these regions of important winter vertical mixing, some of them correspond to well-known convection zones (Gulf of Lions, south Adriatic, north Ionian Sea and Rhodes Gyre). Nevertheless, climatology doesn't represent the extreme values observed in these areas. This is partly due to the spatial and mainly temporal variabilities in the intensity of the convection episodes. For example, convection in the Gulf of Lions reaches certain years its maximum depth in January and other years in February or even in March. Moreover, the decadal variability is believed to be important as a response to the variability of heat losses (Grignon et al., 2010) which would make it difficult to compare our climatology based on a 10-year period to the climatology performed by Houpert et al. (2015) based on a 40-year period. The convection events occurring in the eastern basin present, in the model results, much less interannual variability than in the Gulf of Lions. In the north Ionian and Levantine subbasins, it results in an overestimation of mixing compared to observations presented by Houpert et al. (2015). Not shown time-series in the model presents some high values over 300 m depth in some regions of the eastern basin.

The Algerian basin presents a weak MLD that does not deepen at more than 60 m in winter. In this basin vertical mixing starts in early December and stops in February. A return to stratified conditions is observed in early March. Local spatial variability is observed, which is related to the mesoscale activity. This concerns for example the anticyclonic eddies evolving near the coast.

In the climatology of Houpert et al. (2015), the Alboran Sea is in winter the most stratified region of the Mediterranean. More into details, the Alboran Sea presents a strong mesoscale activity impacting on vertical motion through the northern front near the Spanish coast and the southern anticyclonic West Alboran Gyre (WAG). Our MLD climatology shows an important difference between these two parts of the Alboran Sea. The northern front has a MLD lower than 40 m, all the year while in the anticyclonic WAG the MLD fluctuates between 70 and 90 m depth from December to April.

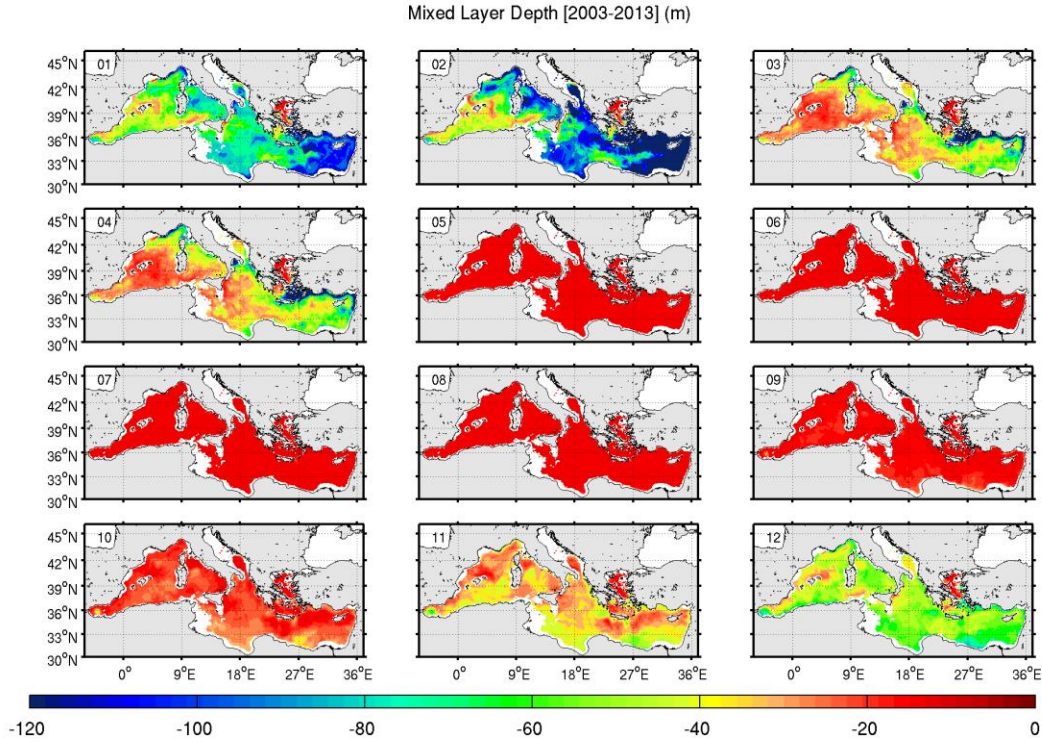


Figure 7: Modeled MLD climatology

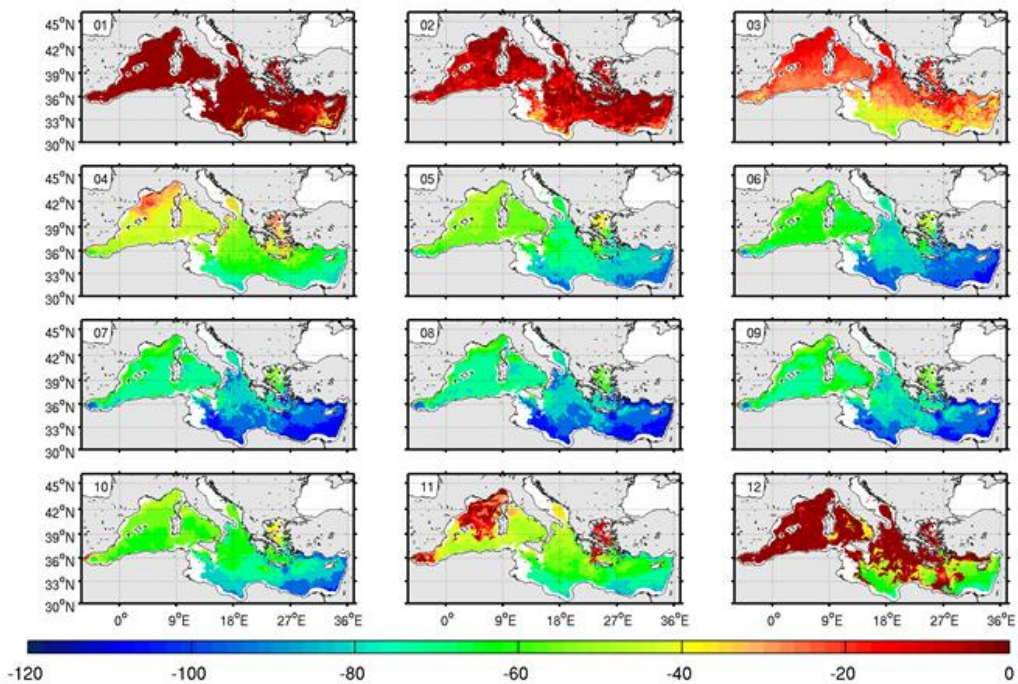
3.2.2 Depth and magnitude of the Deep Chlorophyll Maximum (DCM)

Figure 8 presents the monthly climatology of the depth and magnitude of the model-computed DCM. The chlorophyll maximum is located at the surface in January and February over the entire basin. From March to July, the DCM progressively deepens. This deepening presents a general West-East gradient, characterized by a value of 1.66 m.l^{-1} longitudinal. This estimation is close to the result of Crispi (1999) based on 3D modelling approach and of Lavigne et al. (2015) based on *in situ* observations. Maximal values of DCM depth are reached in July and August, when it attains 60 m in the western and north-eastern subbasins, 90 m in the central eastern basins and 120 m near the south-eastern coast. In autumn, the DCM becomes shallower. In November, the chlorophyll concentration is maximum at the surface in the Alboran Sea, in the north-western region and in the Aegean Sea. Finally in December, the chlorophyll maximum is again located at the surface in the whole basin except in some areas, which are: Tyrrhenian, Ionian and Levantine subbasins. The DCM is therefore present over a wide part of the year, in particular in south-eastern regions. This seasonal cycle of the depth of the DCM is in consistency with the modelling study of Macias et al. (2014).

The DCM presents relatively low concentrations, from October to January. At this period, it is of the order of

0.1-0.2 mg m⁻³ in the south-eastern regions, and of 0.5 mg m⁻³ in the rest of the basin. In spring and summer, maxima (higher than 0.7 mg m⁻³) are visible in the Alboran Sea, north-western region, Adriatic, north-Ionian, and Aegean Seas.

Deep Chlorophyll Maximum Depth [2003-2013] (m)



Mean Deep Chlorophyll Maximum Concentration [2003-2013] ($\mu\text{g/l}$)

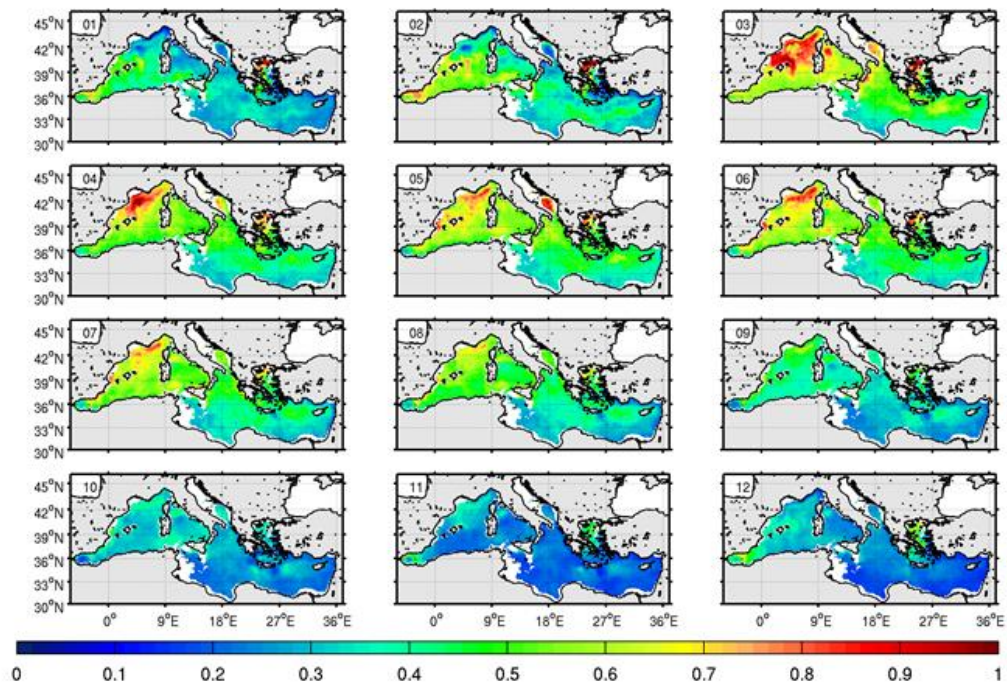


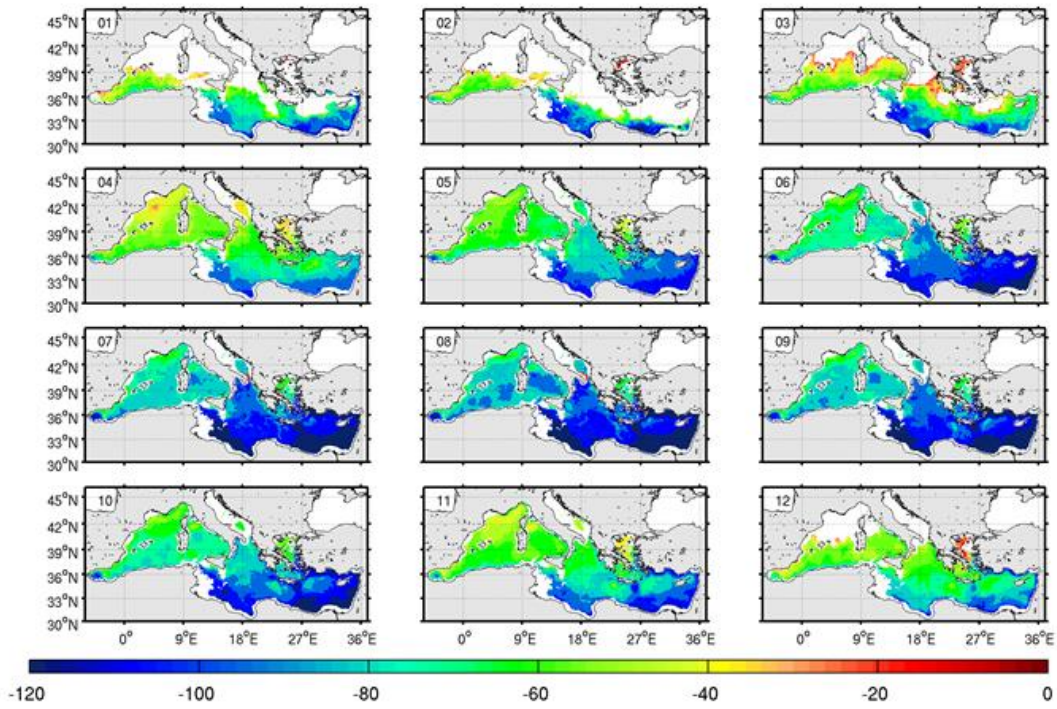
Figure 8: Modeled DCM depth (upper) and chlorophyll maximum concentration (lower) climatologies

3.2.3. Nutriclines

Climatologies of modeled nitracline and phosphocline depths are presented in Fig. 9. West to East and North to South deepening of nutriclines over the basin are globally obtained. Both nutriclines follow the same seasonal evolution. The depths of the top of nutriclines are maximum in August and September. During winter, the nutriclines disappear in the northern parts of the basin, while their depths are minimum in the rest of the basin.

A West-East progressive deepening of phosphocline related to nitracline is also noticeable. The difference of nutriclines depths is maximum in winter in both subbasins. From May to December, this difference is around 8 m in the Levantine subbasin and close to zero in the Algerian subbasin. In February, it is around 50 m in the Levantine subbasin and 10 m in the Algerian subbasin.

Nitracline Depth [2003-2013] (m)



Phosphacine Depth [2003-2013] (m)

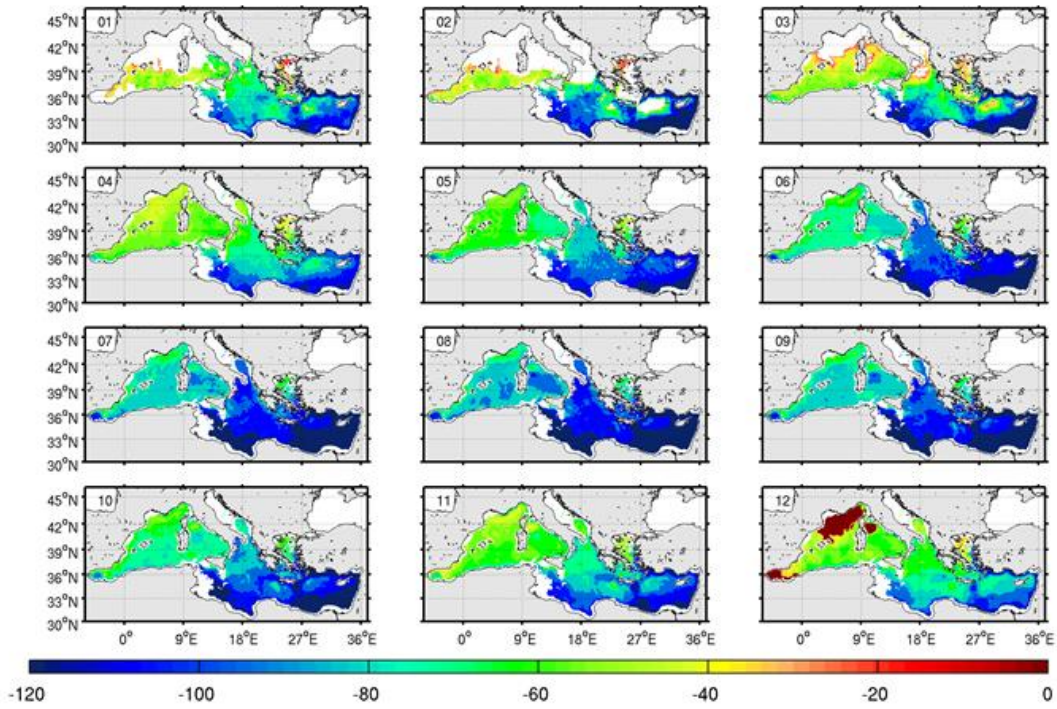


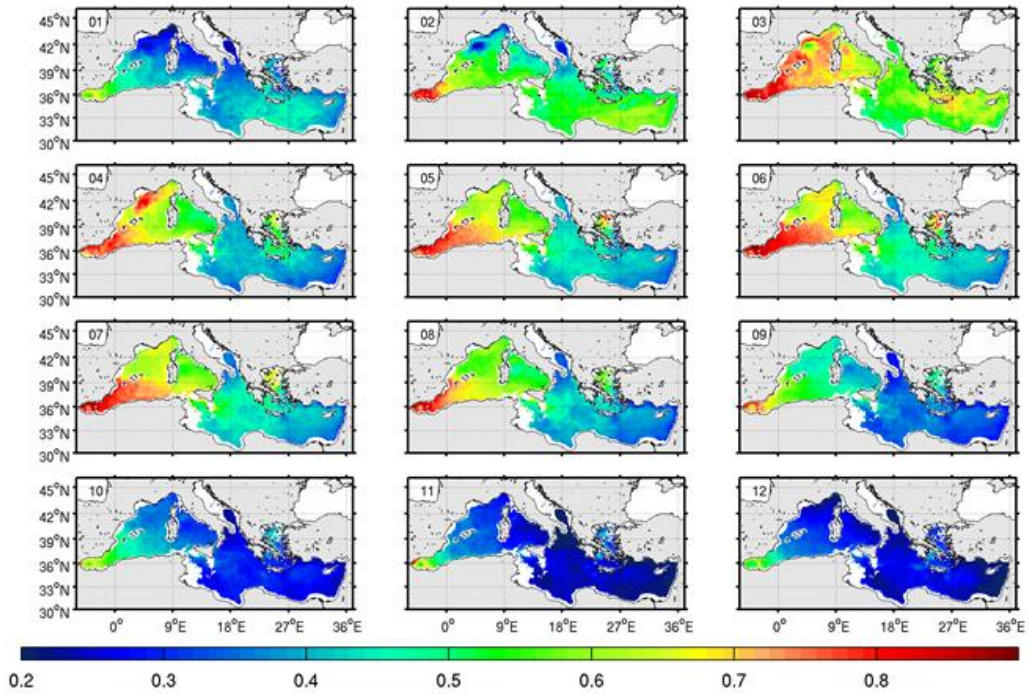
Figure 9: Modeled nitracline (upper) and phosphacline (lower) climatologies

3.2.4. Net primary production (NPP)

The NPP is heterogeneous over the Mediterranean Sea (Fig. 10). Highest values are estimated in the Alboran Sea, where PPN never decreases under $0.5 \text{ gC.m}^{-2}.\text{d}^{-1}$ and attains locally $1 \text{ gC.m}^{-2}.\text{d}^{-1}$ in winter and in spring. At the same time, the WAG contains very lower production which is caused by its anticyclonic circulation. This anticyclone is surrounded by the most productive dynamics of the Mediterranean Sea in a frontal zone. Minima are estimated in the extreme eastern Levantine basin by $0.1 \text{ gC.m}^{-2}.\text{d}^{-1}$ in autumn and $0.4 \text{ gC.m}^{-2}.\text{d}^{-1}$ in winter. The NPP is particularly heterogeneous in the NW, where northern gyre (NG) and the surrounding area show antagonist patterns in winter and spring. In winter, low PPN is simulated in the NG while high values are visible in peripheral zones, and inversely in spring. When the high production triggers, the surrounded waters become less productive. The NPP reaches inside the NG $0.2 \text{ gC.m}^{-2}.\text{d}^{-1}$ in winter and $0.9 \text{ gC.m}^{-2}.\text{d}^{-1}$ in spring. These values are close to estimates from observations described by Uitz et al. (2012).

NPP seasonal evolution is different from the one of the surface chlorophyll concentrations: high production is simulated at the end of spring and beginning of summer (Fig. 10) when the lowest values are simulated and observed for surface chlorophyll (Fig. 4). In the Algerian basin, there is accumulated nutrients in the euphotic layer. During this period, chlorophyll profiles get globally a homogeneous form but some local features such as eddies favor "high surface chlorophyll" (HSC) profiles shape described by (Lavigne et al., 2015) when nutriclines become shallow (not shown).

NET Primary Production [2003-2013] (g/m²/d)



Surface Oxygen Concentration [2003-2013] (ml-mol/m³)

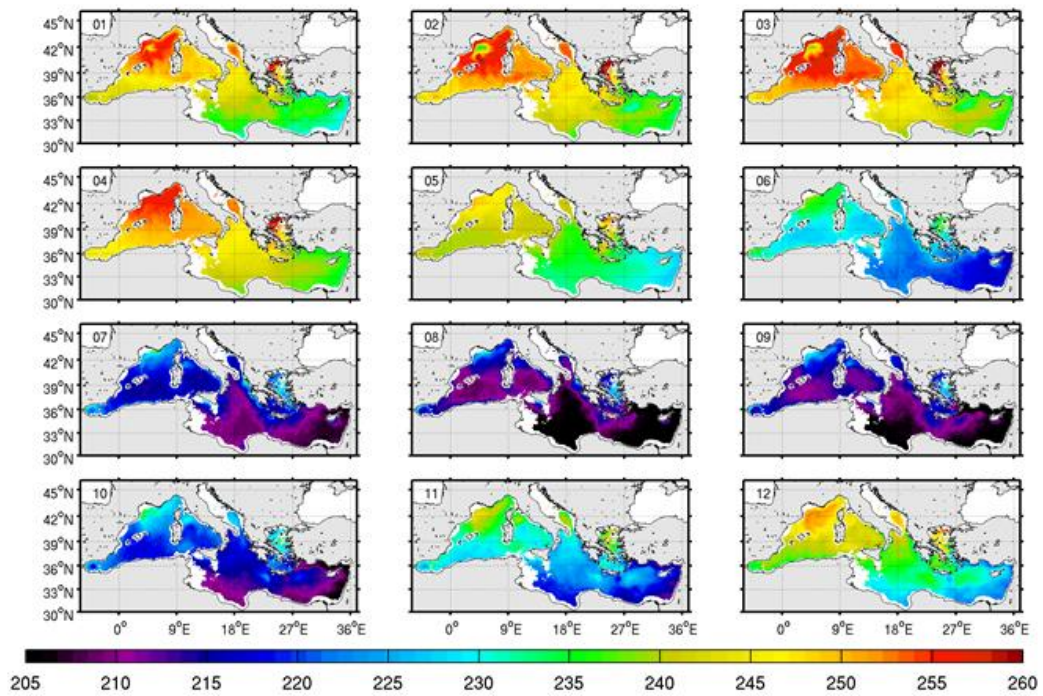


Figure 10: Modeled NPP (upper) and Surface oxygen concentration (lower)
climatologies

3.2.5. Organic carbon export

We have computed the export at 200 m depth because production processes take place above this threshold in the entire basin.

The DOC export (Fig. 11) presents high values [$>20 \text{ mgC}\cdot\text{m}^{-2}\cdot\text{d}^{-1}$] in winter in the northwestern region, north Ionian and the Levantine Seas. The rest of the year it is relatively weak. Some mesoscale features provoking import and export of DOC can be distinguished over the entire basin.

The export of POC (Fig. 11) is high during winter in the whole basin except in the south Ionian and south Levantine subbasins. It ranges between 15 and 25 $\text{mgC}\cdot\text{m}^{-2}\cdot\text{d}^{-1}$ from winter to spring in the NW and Northern Ionian Sea. Maximum export in the NG reaches 100 $\text{mgC}\cdot\text{m}^{-2}\cdot\text{d}^{-1}$ in February and March in the NW. Between May and September, the POC export is about 10 $\text{mgC}\cdot\text{m}^{-2}\cdot\text{d}^{-1}$ in the most productive areas of the NE or NW basins. Meanwhile, SW and SE basins do not show important values in summer and autumn.

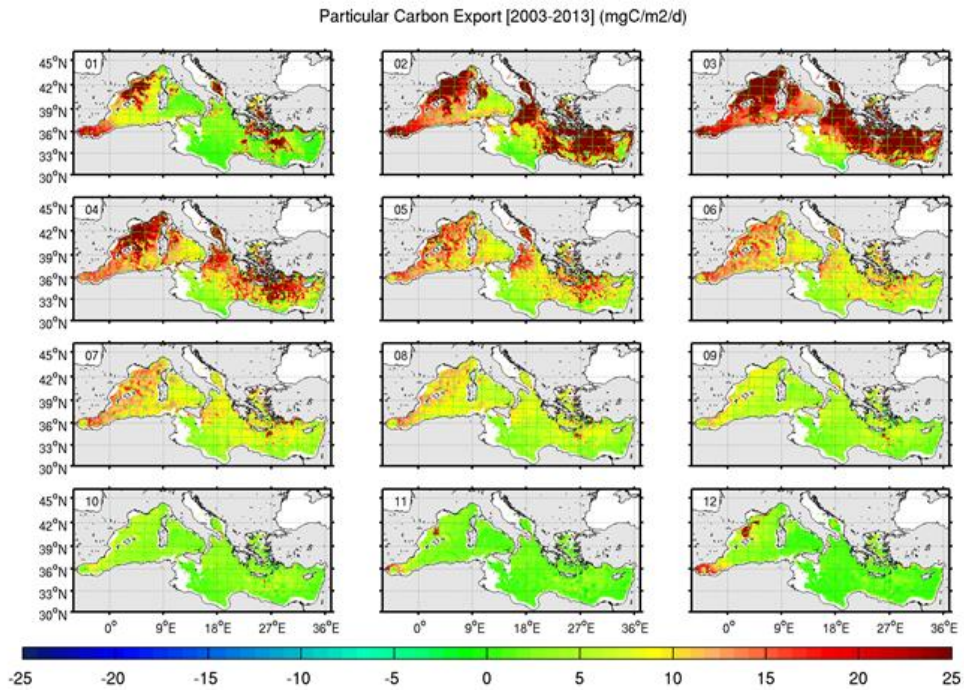
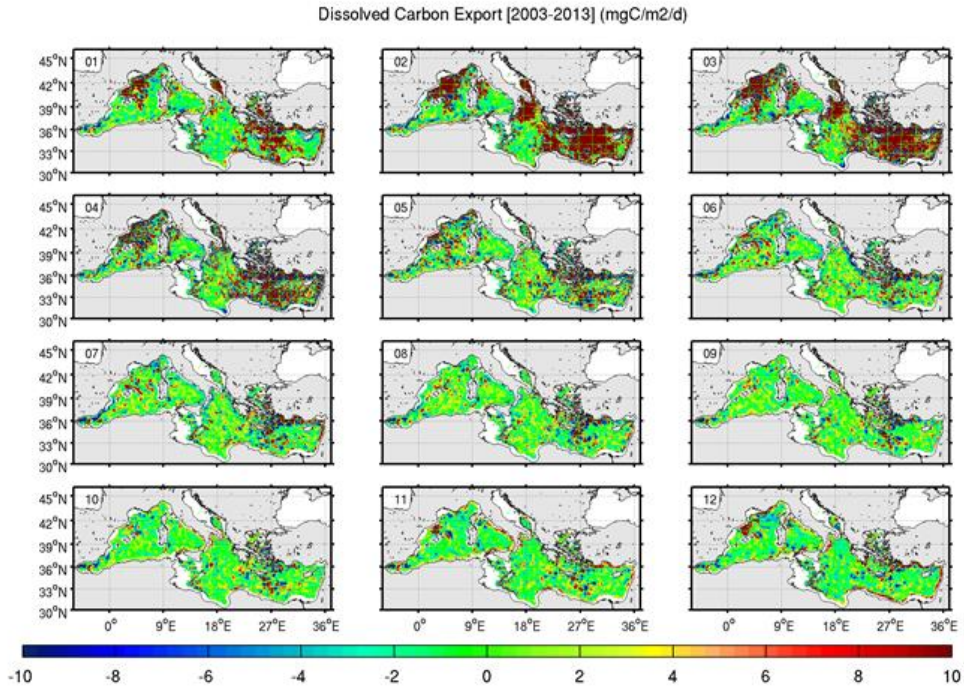


Figure 11: DOC export (upper) and POC export (lower) climatologies

3.3. Main pelagic ecological regimes of the Mediterranean Sea

In the previous section, climatologies of hydrodynamic and biogeochemical variables have been presented in order to gain in understanding of the functioning of the pelagic ecosystem of the Mediterranean Sea. Large spatial heterogeneities have been noticed in both north-south and west-east directions. Here we propose to use a statistical method of clustering to simplify this complex picture and to identify bio-regions characterized by similar seasonal cycles. This objective identification of bioregions is a step forward compared to a fixed division of regions based on geography. Such a regionalization has been proposed for the Mediterranean by D'Ortenzio and Ribera D'Alcalà (2009) from a detailed analysis of the surface chlorophyll seasonal cycle. The different seasonal cycles found with this classification identified different "trophic regimes" present in the classification of Longhurst (1998). They also showed that the structure of the seasonal cycle is tightly coupled with the dynamic range of biomass characterizing the productivity of the region. The idea of repeating this exercise with a model is to have benefit of the large volume of information given by a coupled model not only at the surface but also in the sub-surface as the values of the surface chlorophyll are negligible during a large part of the year although primary production is still active in the DCM.

For clustering, we classified each pixels on the basis of the climatological values of the surface and depth-integrated chlorophyll, the primary production, the nitrate uptake, the amount of nitrate in the upper layer [0-150m], nitrate concentration in the intermediate layer (500 m), the mixed layer depth and the stratification index. Then, for each bioregions we calculated the mean time series. The first three parameters inform about the biological surface and subsurface properties, the nitrate uptake about the ability of phytoplankton to consume nutrients, the amount of nitrate represents the balance between the nutrients imports by vertical dynamics and their consumption and the last parameter characterize the global patterns of the hydrology.

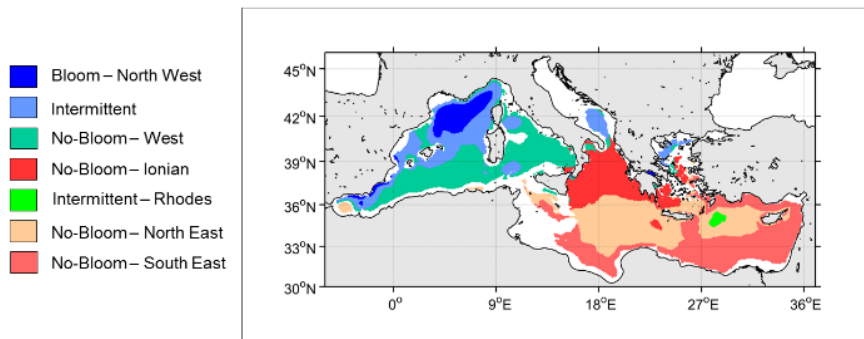


Figure 12: Spatial distribution of bioregions extracted by k-means clustering from physical and biogeochemical datasets derived from the model's outputs.

The k-means clustering using Euclidian distance has been chosen despite the difficulty in the choice of the number of groups. Several tests with different numbers have been performed. The western basin is few sensitive to this number with a final robust repartition in three groups. It is not the case in the eastern basin where the number of groups is sensitive. The choice has been made on a configuration with four specific groups in this basin.

The repartition of these different groups is shown on Fig. 12. The western basin consists of group 1 in the deep northwest basin where dense water formation occurs, group 2 mainly encircling group 1, group 3 in the Algerian and the south Tyrrhenian basins. The eastern basin consists of one group to the north similar to group 2, and 3 groups more or less organized as west east bands. Group 4 is mainly present in the Ionian and Aegean seas, group 5 in the mid Levantine and mid Ionian and group 6 following the southern and eastern coasts of the subbasin. Finally, a small region (group 7) corresponds to the region of the Rhodes gyre. Note also that the anticyclonic West Alboran gyre belongs to group 5. The seasonal cycle of the surface and depth-integrated chlorophyll is given for the different groups in Figure 13.

A comparison with the classification of D'Ortenzio and Ribera d'Alcalà (2009) (DR09) shows some similarities and differences. First, the "Bloom" bioregion of DR09 is very similar to group 1 for the geographical region as well as the surface signature. In the same way, the "Intermittently" bioregion of DR09 has strong similarities with group 2, at the whole periphery of group 1, in the northern Tyrrhenian gyre, in the south Adriatic and along the northern coast of the Alboran Sea. As in DR09, the surface maximum is earlier than in group 1 but it looks more pronounced in the model. The "No Bloom 3" cluster of DR09 could correspond to group 3 although in DR09, it does not extend in the southern Tyrrhenian. The surface chlorophyll cycle presents

differences with DR09: a small peak is present in March and starting from this peak, the simulated concentration decreases too quickly. The eastern basin is dominated in DR09 by two “No bloom clusters”. Our eastern clusters have the same drawbacks than the group 3 cluster of the western basin. In the following, we keep the denomination of DR09 for our clusters even if the No-Bloom denomination could look a little abusive if the small increase of surface chlorophyll in March is considered.

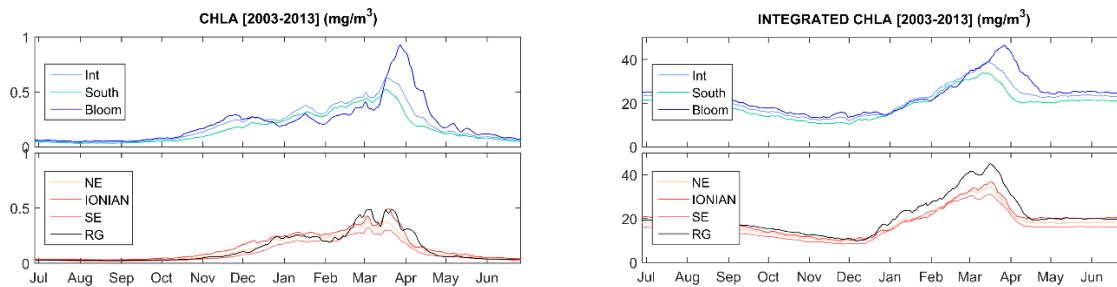


Figure 13: Time-series of surface and integrated chlorophyll climatologies by bioregion (colours mentioned in the maps Fig. 12).

3.3.1. Bloom like regime (group 1)

The first regime corresponds to the “Bloom Like” regime mostly localized in the Northern Gyre (northwestern sub-basin). It is characterized by a strong nutrient enrichment in the surface layer in winter, a temporary accumulation of nutrients in this layer and a huge spring bloom (Fig. 13). In this regime, the DCM disappears progressively starting from December during mixing events and appears again permanently in May (Fig. 14). During winters characterized by deep mixing, surface nutrient concentrations can reach the bottom values. In these cases, the efflorescence is delayed in March-April. The delay of the bloom is caused by winter phytoplankton growth inhibition at the surface caused itself by light limitation when vegetal cells are exported out of the photic layer. Fig.15 indicate that in the NW Bloom box the MLD is much deeper than the nutriclines both positioned at the same depth.

In this region, deep mixing exposes plankton cells and detritus to dilution and favors POC export in January and February. The carbon is also exported under dissolved form as explained by (Santinelli et al., 2010). Winter particulate export is estimated around $25 \text{ mgC.m}^{-2}.\text{d}^{-1}$ on average with much higher values, in mesoscale structures. These values have the magnitude as the sediment traps measurements reported by (Martin et al., 2010). The weak plankton development in winter could appear in contradiction with the strong

export of organic matter. First, a part of the winter export is due to the organic matter produced in the subsurface during autumn. Second, even if the surface biomass concentrations are weak, the depth-integrated biomasses are not negligible (Kessouri et al., in prep-c). Finally vertical mixing and large vertical velocities affecting the whole water column and associated to submesoscale processes in convective regimes favor the export.

In early spring, by the end of the deep mixing period, phytoplankton forms an intense bloom (Fig. 13). In some locations and for some years, chlorophyll concentrations reach more than 2 mg.m^{-3} (not shown) and primary production exceeds $0.9 \text{ gC.m}^{-2}.\text{d}^{-1}$. We expect that the carbon export recorded in spring is associated to the sedimentation of the bloom of large cells. At the end of the bloom, nutriclines (N, P) deepen progressively, but remain vulnerable to occasional gales which characterize this transition period (Bernardello et al., 2012). These gales produce local nutrient enrichment (not shown). Globally, phytoplankton gradually consumes nutrients in the surface layer during one month approximately until depletion. The f-ratio represents the ratio of the new production on total production. The model indicates that the f-ratio in the NW region is in February and March the highest of the basin (after the Adriatic) which is consistent with the strong vertical inputs of nutrients.

Starting in May with the depletion of the surface layer, the DCM progressively deepens to reach its maximum depth in August at 60 m depth. Summer is the period where the f-ratio is minimum indicating the importance of the regenerated production to sustain the production in the DCM. Globally, the net primary production in the northwestern subbasin is not so negligible. The POC export is progressively declining but remains then not negligible. In autumn the DCM starts to rise progressively with the isopycnals between August and the end of November due to wind intensification episodes inducing preconditioning of the northern gyre. The first wind storms inject nutrients in the MLD which progressively thickens. As a consequence the f-ratio increases. This period corresponds to the autumnal bloom.

3.3.2.No-bloom regime of the western basin (group 3)

The No-bloom regime of the western basin concerns the Algerian and Tyrrhenian subbasins. This region, with more than $200\text{-}250 \text{ gC.m}^{-2}.\text{y}^{-1}$, represents in our model the second most productive region of the Mediterranean Sea after the Alboran Sea. The group 3 regime is characterized by regular supplies of nutrient in the surface layer especially between December and February as indicated by the values of the f-ratio, without intense accumulation of nutrients in this layer coupled with a continuous consumption. However, as

already discussed, our model does not reproduce correctly this feature as the surface chlorophyll maximum is found in March while the satellite climatology shows the maximum rather at the end of January, beginning of February (DR09). One explanation could be that the vertical injection of nutrients lasts too long (see intermediate values of the f-ratio in March).

This regime presents the less variable MLD and nutriclines evolutions in the whole Mediterranean (Fig. 14). Two periods emerge from the seasonal cycle:

The first period is the mixing season, from November to March. In both subbasins, the mixing starts during the first autumnal heat losses, from which the DCM begins to shallow. The DCM undergoes a fairly rapid surfacing and disappears in January during the efflorescence.

This regime presents properties close to the Atlantic subtropical gyre where the mixing is rapidly followed by a phytoplankton development. As the model shows, the MLD does not clearly exceed the epipelagic layer. On the other hand, the MLD is close to the nutriclines all along the winter. These characteristics are at the origin of the regular increase of the phytoplankton biomass synchronized with the nutrients inputs. However, it should be noted that the Algerian sub-basin is characterized in winter by the minimum f-ratio of the basin. The vertical input of nutrients seems therefore too low or too irregular to ensure the winter production which could then combine alternations of new and regenerated productions.

The simulation indicates that due to the duration of the efflorescence, the time-integrated productivity is high. A POC export maximum from February to April is associated to this production.

The second period corresponds to the stratified period between April and October. From April, the DCM starts deepening all over the sub-basins to reach in average 55 m depth in summer (Fig. 14). In the center of some local anticyclonic features of the Algerian basin where it could be deeper. Then the DCM remains stable until September. Subsurface water masses contain important phytoplankton concentrations ($0.5 - 0.7 \text{ mg m}^{-3}$) forming a particularly thick DCM (not shown), as mentioned by Lavigne et al., (2015). The Algerian subbasin remains then productive in summer and autumn at subsurface depths. The production is significant in this DCM as the simulated net primary production is $0.7 \text{ gC.m}^{-2}.\text{d}^{-1}$ (between $0.25 - 0.75$ with different satellite based algorithms of primary production of Uitz et al., 2012). The f-ratio is at the minimum value of the basin, 0.18, meaning that 82% of the production is regenerated.

3.3.3. No-bloom regimes of the eastern basin (groups 4, 5, 6)

The eastern basin includes the No-bloom northeastern, southeastern and Ionian bioregions (Fig. 12). It is characterized by deep DCM in summer and weak nitrate supply to the surface. Deep nutrient concentrations are 40% less important than in the western basin.

Two main periods are distinguishable (winter and summer).

In winter, phytoplankton blooming depends on phosphocline depth pierced during mixing events as mentioned by (Lazzari et al., 2012). As shown in Fig. 14, MLD exceeds the phosphocline depths over short periods in February and March for groups 4 and 5. In the no-bloom southeastern regime (group 6), the averaged MLD is never located under the top of the phosphocline. These regimes display low primary production at the beginning of winter. The model overestimates it with values generally in the range $0.45 - 0.55 \text{ gC}\cdot\text{m}^{-2}\cdot\text{d}^{-1}$ between January and March while (Uitz et al., 2012) gave estimates between 0.15 and 0.45. Like in the western no-bloom regime, vertical mixing allows a weak enrichment by nutrients to maintain subsurface phytoplankton production. The new production represents 40 to 50 % of the total production at this period.

During the stratified period, in summer, the DCM reaches its maximum depth. The DCM depth is increasing from west to east. Maximum depth (120 m) is found in the Levantine Sea in August and September (Figs. 8 & 14). Chlorophyll concentration in the DCM is low and decreases from spring to summer from 0.4 to 0.25 mg m^{-3} (Fig. 8). The regenerated production represents about 80% of the total production.

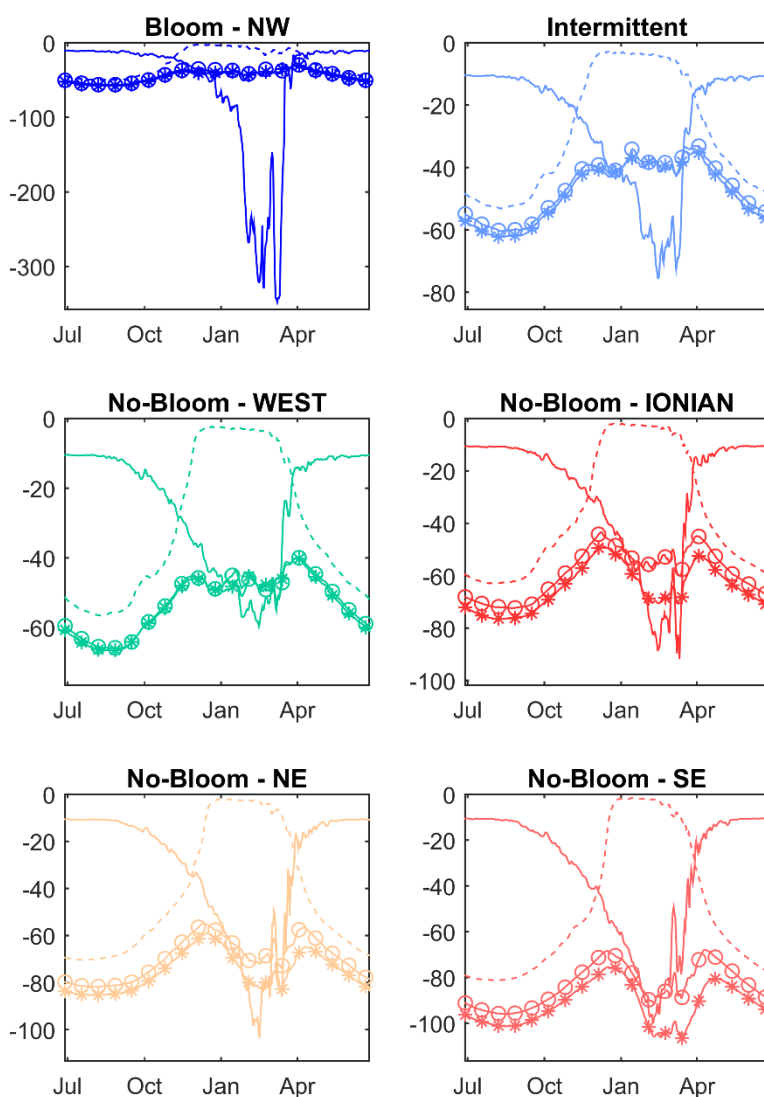
In the no-bloom regimes of the Eastern basin, phosphocline gradually deepens related to the nitracline towards the east. The maximum difference between the phosphocline and nitracline can reach 48 m in the Levantine Sea in February and March. This sub-basin presents the poorest surface and subsurface waters of the Mediterranean in terms of nutrients concentrations and biological activity.

3.3.4. The Intermittent/Intermediate regime (group 2)

This regime characterizes waters surrounding the deep convection area of the northwest Mediterranean as well as regions with moderate to strong mixing (Bonifacio gyre, Adriatic) and stratified regions of the Alboran Sea. The first category is characterized by permanent currents associated to density fronts, as the Northern Current, the North Balearic front where winter mixing can reach 200 m. In the north Alboran Sea, the MLD is

shallow all over the year but the vertical dynamics promoting nutrient enrichment is strong at the periphery of the permanent mesoscale features. Such a variety of regions in this cluster has been also highlighted by DR09.

The common point to these regions is probably an enrichment which is intermediate between the bloom and the no-bloom regimes. This is clear on Fig. 14 where the MLD is significantly deeper than the nutriclines during winter while, first, in the no-bloom regions these interfaces are closer from each other, and, second, in the bloom region, the difference is much larger.



enough to inhibit production (the southern Adriatic should be an exception). Whatever the injection of nutrients is done by convection (Adriatic) or by frontal dynamics (NW and north frontal zone of the Alboran Sea) with immediate consumption. In the first case, the MLD is significantly deeper than in the second one, and in the second case, Figure 14: Climatological time-series of MLD (solid line), DCM (dashed line), nitracline (circles) and the frontal dynamics allows to inject nutrients directly in the MLD.

However, it can be noted an important difference between the two types of regions forming this group. In the

“mixing” regions like the Adriatic, the primary production is apparently lower than in the frontal regions (see Alboran) but a larger part of this production is attributed to new production (maximum f-ratio of 0.66 in February in the Adriatic and only 0.39 in January in Alboran).

The Alboran Sea is very particular. It is the most productive region of the Mediterranean Sea with over 400 $\text{gC}\cdot\text{m}^{-2}\cdot\text{y}^{-1}$. Some regions of this basin are the most productive area of the Mediterranean Sea (Fig. 10), because a high vertical dynamics exist and thus very high NPP is registered every winter in the frontal zone, which is a fine area close to the Spanish coast. According to the classification of (D’Ortenzio and Ribera d’Alcalà, 2009) a northern part of this area could be considered as a “Bloom-like” regime. If we take a comparison to the south, inside the western anticyclonic gyre (WAG), this part is slightly less productive and following our classification, it is considered bio-geochemically too close to the eastern regimes with low production and deep nutriclines (Fig. 12). These remarks are consistent with the time series of (Uitz et al., 2012). All over the year, frontal area in the north is demarcated from the southern part in terms of PPN. POC export is maintained at high values around 15 $\text{mgC}\cdot\text{m}^{-2}\cdot\text{d}^{-1}$ all over the year inside the frontal zone with some pics in winter as higher as those of the NWMed.

The Alboran Sea frontal zone DCM cycle presents two periods. First, between May and October, where the new production inside the DCM is constantly fed by nutrients upwelling. This dynamic is comparable to upwelling zones of Atlantic Subtropical Ocean (Eppley et al., 1981) characterized by winter unimodal chlorophyll profiles (Herbland 1983) or HSC (Lavigne et al 2015) representing maximum chlorophyll at the surface, surrounded by less productive water categorized by “Karabashev” (Herbland, 1983) or “Complex” (Lavigne et al., 2015) chlorophyll profile shape with highly significant values ($> 0.4 \text{ mg/m}^3$) by 40-50 meters. At the same time, constant presence of 500 to 650 $\text{mMolN}\cdot\text{m}^{-2}$ inside the epipelagic layer. During the second part of the year, between November and April, nitrate amount inside the epipelagic layer stays maintained at higher values.

3.4. Nitrogen and phosphorus dynamics in the Mediterranean Sea

3.4.1. Biogeochemical processes

The processes involved in the nitrogen and phosphorus cycles are highlighted within the passage from organic to inorganic forms and vice versa through excretion of inorganic matter and uptake of inorganic

matter. In the model, the excretion of inorganic matter is done by heterotrophs (zooplankton and bacteria) and the absorption of inorganic matter is done by autotrophs and bacteria.

We have divided the western and eastern sub-basins in two layers, surface [0-200m] and deep layer [200m-bottom] and thereby averaging the biogeochemical flux on the ten years of simulation [2003 - 2013].

The result shows that in the western surface layer, organic matter is produced by uptake of nutrients in amounts of $4.1772 \cdot 10^{12} \text{ molN.y}^{-1}$ and $1.7382 \cdot 10^{11} \text{ molP.y}^{-1}$ while nutrients excretion is weaker with $4.0961 \cdot 10^{12} \text{ molN.y}^{-1}$ and $1.698 \cdot 10^{11} \text{ molP.y}^{-1}$. The budget of these two processes is about 2% of the value of the individual processes. In the deep layer, the nutrients uptake are considerably lower ($5.8122 \cdot 10^8 \text{ molN.y}^{-1}$ and $4.6760 \cdot 10^7 \text{ molP.y}^{-1}$) while the nutrients excretion is two orders of magnitude lower than in the surface layer ($5.9487 \cdot 10^{10} \text{ molN.y}^{-1}$ and $4.1017 \cdot 10^9 \text{ molP.y}^{-1}$).

Organic matter production is then larger than nutrients excretion in the western basin by $+23 \cdot 10^9 \text{ molN.y}^{-1}$ and $2.7 \cdot 10^7 \text{ molP.y}^{-1}$.

In the eastern basin, the uptake of nutrients is $7.4625 \cdot 10^{12} \text{ molN.y}^{-1}$ and $1.8091 \cdot 10^{11} \text{ molP.y}^{-1}$ in the surface layer while the nutrients excretion is $7.3395 \cdot 10^{12} \text{ molN.y}^{-1}$ and $1.7349 \cdot 10^{11} \text{ molP.y}^{-1}$. In the deep layer, the uptake is $4.9147 \cdot 10^9 \text{ molN.y}^{-1}$ and $3.6898 \cdot 10^8 \text{ molP.y}^{-1}$ while deep nutrients excretion is $1.7299 \cdot 10^{11} \text{ molN.y}^{-1}$ and $1.1241 \cdot 10^{10} \text{ molP.y}^{-1}$. The functioning of the eastern basin is opposite to the one of the western basin. Nutrients excretion is larger than organic matter production. This can be explained by a stronger export of organic matter under 200 m ($196 \cdot 10^9 \text{ molN.y}^{-1}$ in the eastern sub-basin vs 70 molN.y^{-1} in the western sub-basin), and a lower import of inorganic matter in the surface layer related to organic matter export (50 % in the eastern vs 87 % in the western). An excess of inorganic matter is then produced and a part is exported to the western basin. Figures 16 and 17 present the net budget of nitrogen and phosphorus for each basin.

3.4.2. Fluxes at the straits

Horizontal organic and inorganic fluxes across Gibraltar Strait (GS) and Sicilian Strait (SS) have been extracted daily from the model, then averaged between June 2003 and June 2013. At the GS, the model shows a deep outflow of 0.735 Sv and a surface inflow of 0.782 Sv. Net inorganic matter outflow to the Atlantic is equal to $142 \cdot 10^9 \text{ molN.y}^{-1}$ and $6.6 \cdot 10^9 \text{ molP.y}^{-1}$. This estimation is very close to the one of Huertas et al. (2012) based on observations with $139 \cdot 10^9 \text{ molN.y}^{-1}$ and $4.8 \cdot 10^9 \text{ molP.y}^{-1}$. This budget consists of a deep outflow of inorganic matter of $174 \cdot 10^9 \text{ molN.y}^{-1}$ and $6.6 \cdot 10^9 \text{ molP.y}^{-1}$ and a surface inflow of $34 \cdot 10^9$

molN.y⁻¹ and 1.53 10⁹ molP.y⁻¹. The surface inflow is nevertheless questionable, as nutrients have been forced at 7°W (125 km from GS) using WOA09 monthly climatologies. The nutrients at the surface coming from the Atlantic support the productivity of the Alboran Sea. Nitrate represents 95% of the total inorganic nitrogen flux while ammonium represents 5%. Concerning the organic form, the net inflow at Gibraltar is estimated to 73 10⁹ molN.y⁻¹ and 6.3 10⁹ molP.y⁻¹.

Because of the contrasted biogeochemical functioning of the two basins, important exchanges of inorganic and organic matter take place at the SS between the eastern and western basins (see chlorophyll at longitude~11°E in Fig. 7). A deep flow directed from the east to the west of 1.0055 Sv is the main vector of a net nutrient flux of 86 10⁹ molN.y⁻¹ and 3.88 10⁹ molP.y⁻¹, close to the estimations of Huertas et al. (2012) of 92 10⁹ molN.y⁻¹ and 4.1 10⁹ molP.y⁻¹. The surface eastward flow of 0.9508 Sv is enriched in organic matter and is the main vector of the net eastward flux of 78 10⁹ molN.y⁻¹ and 4 10⁹ molP.y⁻¹.

3.4.3. The global budget

Before discussing the budget, the evolution of the nutrients stocks is important to judge of the model stability. Compared to the state of 2003, the inorganic nitrogen in 2013 presents a mean deficit of 36 10⁹ molN.y⁻¹ in the western basin and a gain of 38 10⁹ molN.y⁻¹ in the eastern basin, while the total stock is equal to about 1.1043 10¹³ molN in the western basin and 1.1268 10¹³ molN in the eastern basin. This annual variation represents 0.3% of the stock of each sub-basin and is very low for the entire basin. The accumulation of nutrients in the eastern basin and the deficit in the western basin may have different combined causes. A too high export of organic matter from the western basin to the eastern basin due to an incorrect positioning of the depths of remineralization of organic matter, itself a compromise between the sedimentation velocity of organic matter and its decomposition rate could be a good candidate. This is compatible with the loss of nutrients in the western basin which affects the [300 - 1200 m] layer (not shown) while the accumulation in the eastern basin affects the [130 - 400 m] layer. On the other hand, biases in the general circulation including the exchanges at the straits and convection intensity could also participate to this imbalance. We can finally note that the subsurface accumulation of nutrients to the east could be responsible of the too high production suggested by the comparison of chlorophyll with satellite (Fig. 4).

Despite these imbalances, some conclusions can be drawn from this budget.

The western basin is more productive than the eastern one as long as the uptake and the excretion rate by surface unit are compared. The simulated uptake is 5.22 and 4.66 molN.m⁻².y⁻¹ for the western and eastern basins respectively while the excretion is 5.1 and 4.59 molN.m⁻².y⁻¹.

The western basin seems to be responsible of a large transfer of organic matter to the eastern basin (even if it could be overestimated as discussed above). A large flux of organic matter entering into the western basin has been found throughout the Gibraltar Strait representing half the outflow of inorganic nitrogen and the total outflow of inorganic phosphorus. This imbalance of these two elements reflects the increase of the N:P ratio along the path of the water in the Mediterranean basin. Besides, the inorganic matter flux from the eastern basin to the western basin has been found equal to 60% of the outflow to the Atlantic meaning that the western basin contributes by 40% to the outflow at Gibraltar.

In our simulation, the amount of nutrients coming from the rivers (Ludwig et al., 2010) and Black Sea (Tugrul et al., 2002) is estimated equal to 47 % (23 %) of the inorganic nitrogen (resp. phosphorus) exported throughout Gibraltar, which gives to the river inputs an important role in the global budget of the Mediterranean Sea. Finally, atmospheric inputs are not negligible in the global budget of the Mediterranean.